

5. CGS4 is a cryogenic grating spectrometer containing a two-dimensional array of InSb photodiodes, usable in the 1- to 5- $\mu\text{m}$  wavelength band at resolving powers between 200 and 20,000. UKIRT is operated by the Royal Observatory Edinburgh on behalf of the United Kingdom Science and Engineering Research Council. Triton spectra were obtained on 29 June 1991 (comparisons stars BS 7340 and BS 6965), 18 October 1991 (comparison star BS 7340), 5 May 1992 (poor data) and 27 and 28 May 1992 (comparison stars BS 6998 and BS 7504) (presented here in Fig. 1). Additional data showing the  $\text{N}_2$  band at higher resolution (from which the wavelengths given in the text are derived) were obtained on 22, 23, and 24 September 1992. All dates in universal time.

6. B. Hapke, *J. Geophys. Res.* **86**, 3039 (1981); *Icarus* **59**, 41 (1984); *Icarus* **67**, 264 (1986).

7. T. L. Roush, J. B. Pollack, F. C. Witteborn, J. D. Bregman, J. P. Simpson, *Icarus* **86**, 355 (1990).

8. B. Schmitt, E. Quirico, E. Lellouch, *Proc. Symp. Titan, ESA SP-338*, 383 (1992); J. R. Green, R. H. Brown, D. P. Cruikshank, *Bull. Am. Astron. Soc.* **23**, 1208 (1991); G. B. Hansen, *Appl. Opt.* **25**, 2650 (1986); S. G. Warren, *Bull. Am. Astron. Soc.* **24**, 978 (1992). In our modeling we derive the radiance factor at zero degrees phase angle ( $i = e = 0$  degrees). We assume isotropic surface scattering, a lunar-like regolith parameter for Hapke's  $h$ -value, and we make no corrections for macroscopic surface roughness. The continuum is defined as a series of straight line segments connecting local maxima such that data between maxima are not cut by the continuum. This has the effect of eliminating absolute albedo information. However, preliminary calculations of geometric albedos for these mixtures are entirely consistent with the values derived from the telescopic data. We shifted the optical constant values to agree with the observational data (1992 smoothed data) prior to calculation of the spectra.

9. B. Schmitt *et al.*, *Bull. Am. Astron. Soc.* **22**, 1121 (1990) (abstract). The  $\text{CH}_4$  fraction has been changed since publication of this abstract and is now "between 0.05 and 0.5%." A more extensive paper has been submitted to *Icarus*.

10. A. L. Broadfoot *et al.*, in (2); G. L. Tyler *et al.*, *Science* **246**, 1466 (1989).

11. L. Trafton, *Icarus* **58**, 312 (1984).

12. The wavelength calibration of the CGS4 spectrometer is determined from emission-line lamps and is accurate to 0.0001  $\mu\text{m}$  (one sigma).

13. The presence of  $\alpha\text{-N}_2$  is unexpected on Triton because the surface temperature (if it is in fact in strict vapor pressure equilibrium with the atmosphere at  $P_s = 16 \mu\text{bar}$ ) is 37.7 K. The uniform temperature predicted by Trafton (11) further argues against coexistence of surface exposures of the  $\alpha$  and  $\beta$  phases. In addition, although the phase transition temperature in  $\text{N}_2$  is raised when the nitrogen is contaminated with CO or  $\text{CH}_4$  [T. A. Scott, *Phys. Rep.* **27** (no. 3), 89 (1976)], the concentrations of the contaminants implied by our spectra are too low to raise the transition temperature at least the 2 K required. Nevertheless, physical studies of solid  $\text{N}_2$  contaminated with  $\text{CH}_4$  and near the 35.6 K phase transition temperature show that the  $\text{N}_2$  in close proximity to a  $\text{CH}_4$  molecule is in the  $\alpha$  phase, while that further away from a contaminant molecule is in the  $\beta$  phase. Thus, a mixed  $\alpha$ - $\beta$  spectrum may result.

14. J. Eluszkiewicz, *J. Geophys. Res.* **96**, 19,219 (1991).

15. T. C. Owen *et al.*, *Int. Astron. Union Circ.* **5532** (1992).

16. F. Herbert and B. R. Sandel, *J. Geophys. Res.* **96**, 19,241 (1991).

17. The shifting of the bands of  $\text{CH}_4$  diluted in  $\text{N}_2$  is not related simply to the concentration. In particular, the band at 2.324- $\mu\text{m}$  shifts slightly and then splits as the  $\text{CH}_4$  concentration is reduced; eventually the "pure" component diminishes as the 2.311- $\mu\text{m}$  component dominates.

18. S. A. Sandford, L. J. Allamandola, A. G. G. M. Tielens, G. J. Valero, *Astrophys. J.* **329**, 498 (1988).

19. Transmission spectra of molecular mixtures of CO

in  $\text{N}_2$  show that the matrix shift of the CO overtone band at 2.351  $\mu\text{m}$  is approximately  $-0.0006 \mu\text{m}$ , or about  $1 \text{ cm}^{-1}$ . This result was confirmed by D. Hudgins at Ames Research Center.

20. G. N. Brown, Jr., and W. T. Ziegler, *Adv. Cryog., Eng.* **25**, 662 (1979).

21. M. H. Stevens *et al.*, *Geophys. Res. Lett.* **19**, 669 (1992); V. A. Krasnopolsky *et al.*, *J. Geo-*

*phys. Res.* **98**, 3065 (1993).

22. We thank Douglas Hudgins for his laboratory work on the  $\text{N}_2 + \text{CO}$  spectrum. We also thank the staff of the United Kingdom Infrared Telescope Facility for their support during the observations reported here.

12 January 1993; accepted 16 April 1993

## Surface Ices and the Atmospheric Composition of Pluto

Tobias C. Owen,\* Ted L. Roush, Dale P. Cruikshank, James L. Elliot, Leslie A. Young, Catherine de Bergh, Bernard Schmitt, Thomas R. Geballe, Robert H. Brown, Mary Jane Bartholomew

Observations of the 1.4- to 2.4-micrometer spectrum of Pluto reveal absorptions of carbon monoxide and nitrogen ices and confirm the presence of solid methane. Frozen nitrogen is more abundant than the other two ices by a factor of about 50; gaseous nitrogen must therefore be the major atmospheric constituent. The absence of carbon dioxide absorptions is one of several differences between the spectra of Pluto and Triton in this region. Both worlds carry information about the composition of the solar nebula and the processes by which icy planetesimals formed.

Although Pluto is usually classified as a planet, its closest relative in the solar system appears to be Triton, Neptune's largest satellite. Both of these objects evidently formed from the solar nebula at a distance of  $\sim 40$  astronomical units (AU) from the sun, where temperatures were  $< 50$  K. In this respect, they may be considered huge icy planetesimals that somehow escaped accretion by the giant planets. The lower end of the mass distribution of such objects is represented by the common comets, objects 2060 Chiron, 5145 Pholus, 1992 QB1, and the great comet of 1729 (1). These objects represent an especially primitive stage in the transition from the grains and gas of interstellar clouds to the planets and satellites of the solar system.

We have presented observations of the near-infrared spectrum of Triton (2). We used the same instrumental configuration to study Pluto, without the benefit of Voyager data to provide a context for our work. It is the only planet not yet visited by spacecraft, but its recent occultation of a star (3) and the mutual eclipses and occultations exhibited by Pluto and its synchronously orbiting satellite Charon (4) have helped to define this distant system (5).

Using the cooled grating array spectrometer with the United Kingdom Infrared Telescope, we recorded Pluto's spectrum from 1.4 to 2.4  $\mu\text{m}$  ( $4160$  to  $7140 \text{ cm}^{-1}$ ) at a resolution of 350 on 27 and 28 May 1992 (UT) (6). Previous observations at lower resolution had established that there is solid  $\text{CH}_4$  on Pluto's surface (7). Our spectra confirmed the presence of this ice, revealing the same series of strong  $\text{CH}_4$  bands seen on Triton. In addition, the (2,0) band of CO at 2.35  $\mu\text{m}$  and the  $\text{N}_2$  absorption at 2.15  $\mu\text{m}$  were added, both of which are also present in Triton's spectrum (2) (Fig. 1).

Despite these general similarities, the spectra of Pluto and Triton are not identical. We do not find the solid  $\text{CO}_2$  absorptions on Pluto that are so prominent on Triton. In particular, the absence of the strong triad of  $\text{CO}_2$  bands near 2.0  $\mu\text{m}$  (2) means that the amount of this ice on Pluto must be less than one-third of the amount that forms the spectrum of Triton. The shapes of the  $\text{CH}_4$  bands in the region from 2.0 to 2.4  $\mu\text{m}$  are broader and deeper on Pluto, whose spectrum exhibits an additional  $\text{CH}_4$  feature at 1.48  $\mu\text{m}$  that is not

T. C. Owen, Institute for Astronomy, University of Hawaii, 2680 Woodlawn Drive, Honolulu, HI 96822.  
 T. L. Roush, Department of Geosciences, San Francisco State University, San Francisco, CA 94132, and NASA Ames Research Center, Space Sciences Division, Moffett Field, CA 94035-1000.  
 D. P. Cruikshank, NASA Ames Research Center, Space Sciences Division, Moffett Field, CA 94035-1000.  
 J. L. Elliot and L. A. Young, Department of Earth, Atmospheric and Planetary Sciences, Massachusetts Institute of Technology, Cambridge, MA 02139.  
 C. de Bergh, Observatoire de Paris, 92195 Meudon Cedex, France.  
 B. Schmitt, Laboratoire de Glaciologie et Geophysique de l'Environnement, 38402 St. Martin d'Hères, France.  
 T. R. Geballe, Joint Astronomy Centre, Hilo, HI 96720.  
 R. H. Brown, Jet Propulsion Laboratory, Pasadena, CA 91109.  
 M. J. Bartholomew, Sterling Software, Inc., NASA Ames Research Center, Moffett Field, CA 94035-1000.

\*To whom correspondence should be addressed.

present on Triton (Fig. 2). Another  $\text{CH}_4$  band of comparable strength in the laboratory (at  $1.68 \mu\text{m}$ ) does not appear in the spectrum of either Pluto or Triton. This difference in appearance of the  $\text{CH}_4$  absorptions must carry some information about a difference in temperature, composition, or average grain size on the surfaces of Pluto and Triton. Unfortunately, the laboratory data are not yet adequate to determine this difference.

The  $\text{N}_2$  feature at  $2.15 \mu\text{m}$  is distinctly weaker on Pluto than on Triton; there is a hint of an accompanying absorption at  $2.16 \mu\text{m}$  (Fig. 1). The association of this feature with  $\text{N}_2$  is confirmed by the fact that its strength has the same proportion to the primary  $2.15\text{-}\mu\text{m}$   $\text{N}_2$  absorption as in the spectrum of Triton (2). Further study of this band should help to place better constraints on the poorly defined surface temperature of Pluto (8) because the relative intensity of the  $2.16\text{-}\mu\text{m}$  feature is strongly temperature-sensitive (9).

At the scale of the entrance slit of the spectrometer, Pluto and its satellite Charon are not resolved into individual objects, so the resulting spectrum is a composite of the contributions of each. The spectrum of Charon is known to exhibit absorption from  $\text{H}_2\text{O}$  ice (10, 11). At a given wavelength, Charon's contribution to the combined spectrum with Pluto is weighted by the relative areas of the two bodies and by the geometric albedos of their surfaces. From the mutual eclipses and transits of Pluto and Charon observed in the 1980s, we adopt the radii of Pluto and Charon as 1142 and 596 km, respectively. The area ratio of Pluto to Charon is then 3.67, with Charon's contribution as 27% of the total (12).

We have modeled the Pluto spectrum

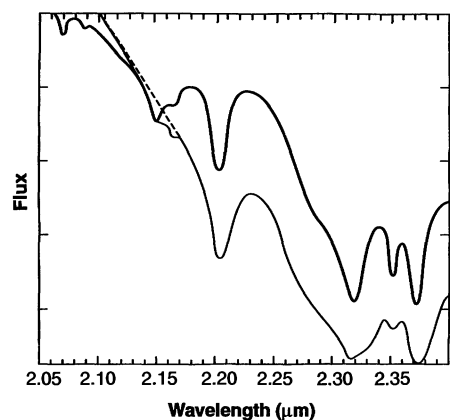


**Fig. 1.** Smoothed spectra of Triton (heavy trace) and Pluto (light trace) are shown in the region from 2.1 to  $2.4 \mu\text{m}$ . The dashed line in the Pluto spectrum indicates the continuum in the region of  $\text{N}_2$  absorption. Absorption from ices of  $\text{N}_2$  ( $2.15 \mu\text{m}$ ),  $\text{CH}_4$  ( $2.2$ ,  $2.32$ , and  $2.38 \mu\text{m}$ ), and  $\text{CO}$  ( $2.35 \mu\text{m}$ ) are apparent.

using the same basic approach we applied to Triton (2, 13). The model consists of an intimate mixture (a salt-and-pepper configuration) of  $\text{N}_2$ ,  $\text{CH}_4$ , and  $\text{CO}$  ices to represent Pluto, plus a spatially segregated area of  $\text{H}_2\text{O}$  ice representing Charon's contribution to the spectrum (Fig. 2). The  $\text{H}_2\text{O}$  spectrum used for Charon's contribution was computed separately on the basis of scattering theory with the use of the Charon spectrum of Buie and colleagues (11) and optical constants of the pure ices (14). Absorption bands of  $\text{H}_2\text{O}$  ice in the wavelength region of interest are broad ( $0.1$  to  $0.3 \mu\text{m}$ ), and in the model they principally affect the shape of the continuum on which the narrower bands of  $\text{CH}_4$ ,  $\text{N}_2$ , and  $\text{CO}$  are superimposed. In the present case, the  $\text{H}_2\text{O}$  ice that is included as a spatially segregated component in the model spectrum most strongly affects the regions from  $1.45$  to  $1.55 \mu\text{m}$  and from  $2.10$  to  $2.30 \mu\text{m}$ . The effect of the  $\text{H}_2\text{O}$  ice is not evident in the observed spectrum of Pluto plus Charon; our calculated spectrum is too low at  $1.5 \mu\text{m}$  and too high at the longer wavelengths.

As in the case of Triton, we find that  $\text{N}_2$  is the most abundant surface ice on Pluto. The abundances of  $\text{CH}_4$  and  $\text{CO}$  are greater on Pluto than on Triton but are still small relative to that of  $\text{N}_2$ . As in the case of Triton, Pluto's  $\text{CH}_4$  bands are shifted from their laboratory-measured wavelengths, demonstrating that  $\text{CH}_4$  and  $\text{N}_2$  must be mixed at the molecular level to form a solid solution. A checkerboard or salt-and-pepper model for the surface distribution of the two ices does not help to explain the observed wavelengths of the  $\text{CH}_4$  bands. Thus, the intimate mixture (salt-and-pepper) model we have used (Fig. 2) is not correct but is the best we can do with available laboratory data for the optical constants of these ices (15). As noted in our discussion of Triton's spectrum (2), the shifting of the  $\text{CH}_4$  bands is a complex phenomenon related to the concentration in the solvent ( $\text{N}_2$ ) that affects not only the

central wavelength but the shape of the bands as well. Furthermore, the various  $\text{CH}_4$  bands in this spectral region behave differently from one another (16). In the case of our model of Pluto's spectrum, the derived abundance of  $\text{CH}_4$  (1.5%) is consistent with the degree of shift of the bands. This consistency means that  $\text{CH}_4$  ice is more abundant on the surface of Pluto than on Triton, where it is  $\sim 0.05\%$  (2). The exact abundance will be more reliably derived from models that incorporate optical constants of true molecular mixes of  $\text{N}_2$  and  $\text{CH}_4$  when they become available. The present uncertainty in the  $\text{CH}_4$  abundance as determined from our models is a factor of 2.

We modeled the  $\text{CO}$  in Pluto's spectrum using only the (2,0) band at  $2.352 \mu\text{m}$ , although the weaker (3,0) band at  $1.578 \mu\text{m}$  may also be marginally present on the short wavelength slope of a  $\text{CH}_4$  band. As in the case of Triton, we cannot establish whether the  $\text{CO}$  is present as individual grains or dissolved in a molecular mixture with  $\text{N}_2$  and  $\text{CH}_4$ , because the wavelength shift of  $\text{CO}$  that results from matrix effects is below the resolution limit of our Pluto spectrum. The similarities in the vapor pressures of  $\text{CO}$  and  $\text{N}_2$  suggest that these ices are mixed at the molecular level, but there is no independent information from the planet's atmosphere or surface to help resolve this question. If  $\text{CO}$  is present as individual grains of ice, the particle sizes cannot be extremely small because of the quenching effect that small grains would have on the strength of the  $\text{N}_2$  band. In our best fitting model, the abundance and grain size of  $\text{CO}$  are 0.5% and 0.5 mm, respectively, again with a factor of 2 uncertainty.

There are several conclusions we can draw from this coupled set of observations of these two frigid worlds. The first involves Pluto's atmosphere. If we assume that  $\text{CH}_4$ ,  $\text{CO}$ , and  $\text{N}_2$  are the only volatiles on Pluto, that the ices are in ideal solutions, and that the atmospheric composition is determined simply by vapor-ice equilibrium, then the partial pressures are  $P_i = X_i V_i$ , where  $X_i$  is

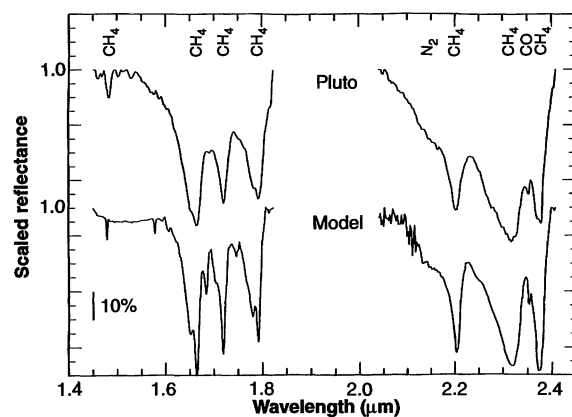


**Fig. 2.** A comparison of a continuum-adjusted spectrum of Pluto and a model spectrum based on the indicated mixture of ices over the wavelength range of  $1.4$  to  $2.4 \mu\text{m}$ . This model is an intimate mixture of the components rather than the expected molecular mixture.

the mole fraction on the surface (0.026, 0.005, and 0.969 for CH<sub>4</sub>, CO, and N<sub>2</sub>, respectively) and V<sub>i</sub> is the vapor pressure of the i<sup>th</sup> gas over its pure ice (17). Thus, using the surface temperature, the observed mixing ratios in the solid, and the known vapor pressures (18) we can find the partial pressure and the atmospheric mixing ratio q<sub>i</sub> for each gas. Unfortunately, Pluto's surface temperature is not well determined: published values range from 31 K to 59 K, depending on the observations used and the different assumptions of the surface properties, especially the solar phase integral and emissivity (8). We have constructed Table 1 for three representative temperatures. For each temperature and volatile there is a tabulated vapor pressure over pure ice, partial pressure in the atmosphere, and mixing ratio in the atmosphere.

We can tightly constrain the possibilities for the surface temperature and pressure by combining our inferences about the atmospheric composition with the constraints imposed by the 1988 stellar occultation. The data in Table 1 demonstrate that for all temperatures, the atmosphere is >99% N<sub>2</sub>, close to the 100% N<sub>2</sub> atmosphere considered by Elliot and Young (19). The absence of near-surface haze would suggest a surface radius of 1206 ± 11 km, a surface temperature of 35.3 ± 0.4 K, and a surface pressure of 3.3 ± 0.8 μbar. This temperature is close to 35.62 K, the triple point of vapor, alpha, and beta N<sub>2</sub>. The presence of a near-surface haze would decrease the surface radius, with a corresponding increase in surface temperature and pressure.

Although our discovery of N<sub>2</sub> and CO substantiates the suggestion by Yelle and Lunine (20) that a gas heavier than CH<sub>4</sub> is present in Pluto's atmosphere, the amount of CH<sub>4</sub> gas that we infer is less than the 0.1% apparently required by their model to maintain the lower atmosphere at 106 K. However, their model has already survived some observational tests. It predicts that

**Table 1.** Vapor pressures, partial pressures, and mixing ratios for gases in Pluto's atmosphere.

Gas	V (μbar)	P (μbar)	q
T = 34 K			
CH <sub>4</sub>	4.4 × 10 <sup>-5</sup>	1.1 × 10 <sup>-6</sup>	9 × 10 <sup>-7</sup>
CO	5.9 × 10 <sup>-2</sup>	2.9 × 10 <sup>-4</sup>	2 × 10 <sup>-4</sup>
N <sub>2</sub>	1.3	1.2	1
T = 45 K			
CH <sub>4</sub>	0.21	5.5 × 10 <sup>-3</sup>	9 × 10 <sup>-6</sup>
CO	92	0.46	8 × 10 <sup>-4</sup>
N <sub>2</sub>	610	590	1
T = 58 K			
CH <sub>4</sub>	77	2	5 × 10 <sup>-5</sup>
CO	1.4 × 10 <sup>4</sup>	70	2 × 10 <sup>-3</sup>
N <sub>2</sub>	3.9 × 10 <sup>4</sup>	3.8 × 10 <sup>4</sup>	1

the atmospheric temperature profile should be isothermal with altitude, which has been established from the Kuiper Airborne Observatory occultation data (19) for a zone that begins ~10 km above the surface (or haze layer) and extends upward for several scale heights (21). At those altitudes, under the assumption of 100% N<sub>2</sub> (19), the atmospheric temperature is 104 ± 21 K. The agreement of this observationally derived value with Yelle and Lunine's prediction may mean that even less CH<sub>4</sub> than they proposed is needed to raise the temperature or that there is another way of increasing the CH<sub>4</sub> vapor pressure in the atmosphere than by sublimation from surface frosts. An atmospheric heating source other than CH<sub>4</sub> (such as aerosols) may also be at work.

The role of CH<sub>4</sub> heating is significant to an understanding of the difference between the atmospheric models for Pluto and Triton, which results from the amount of CH<sub>4</sub> in each atmosphere. For Triton, the amount of CH<sub>4</sub> (as determined by Voyager observations) is too low for radiative processes to affect the energy balance significantly (22). However, in the current model for Pluto radiative absorption and reemission by CH<sub>4</sub> set the energy balance at 106 K (20). A test of the CH<sub>4</sub> atmospheric abundance that we have inferred from the surface ice spectra will come from an observational study of CH<sub>4</sub> gas absorption in Pluto's atmosphere (23).

As on Triton, Pluto shows no evidence of other ices; we found the same list of absent ices on that planet. In one respect, this absence is even more puzzling than for Triton because Pluto is darker and exhibits a 0.3-magnitude (~30%) variation in brightness as it rotates, indicating an inhomogeneous surface. If the general similarity of Pluto's spectrum to that of Triton is at all diagnostic of surface conditions on these two bodies, we expect thicker, more widespread deposits on Pluto of dark material similar to the isolated patches the Voyager cameras revealed on Triton. This expectation carries with it the idea that intermediate products in the chemical reactions leading from CH<sub>4</sub> and N<sub>2</sub> to this dark material should be present. Evidently their concentration is extremely low.

The relatively high abundance of molecular N<sub>2</sub> on Pluto and Triton supports the widely held hypothesis that the missing (that is, unobserved) 70% of the cosmic abundance of N<sub>2</sub> expected in the interstellar medium (ISM) is in the form of N<sub>2</sub> (24). The low abundance of N<sub>2</sub> in Halley's Comet (25) could then be understood to result from sublimation and desorption of an original endowment of N<sub>2</sub> (26). The low relative abundance of CO on Pluto and Triton poses a problem, however. From ISM abun-

dances, one expects the CO/N<sub>2</sub> ratio to be ~1. Evidently some combination of the partial processing of CO to CH<sub>4</sub> and CO<sub>2</sub> during accretion [following pathways demonstrated in the laboratory (27)] with subsequent layering on the surface according to vapor pressure led to the presently observed state. From this view, the absence of observable CO<sub>2</sub> on Pluto, in contrast to Triton, resulted from the current difference in the general circulations of the atmospheres of these two bodies, corresponding to the different inclinations of their rotational axes. On Triton, the flight of N<sub>2</sub> from the sunlit southern hemisphere could have exposed underlying CO<sub>2</sub> to view. Observations over the next few decades could easily test this model if the circulation pattern on Pluto changes sufficiently before the atmosphere simply freezes out.

Finally, the amount of neon in the atmospheres of these objects is important because the cosmic abundance of this element is about equal to that of N<sub>2</sub> (28) and its vapor pressure is 5 × 10<sup>6</sup> the pressure of neon at 35 K. Neon should therefore dominate these atmospheres, although on Triton this is clearly not the case (29). If neon were so abundant, there would be a lower mean molecular weight on Pluto from occultation observations than the value corresponding to 99% N<sub>2</sub> (Table 1) (30). If Triton and Pluto formed at temperatures above 20 K, neon would not have been trapped in the constituent water ice (31) and would therefore not be expected in their two atmospheres.

We now only have observations of one hemisphere of this variegated planet. Future investigations may reveal some spectral signature that could help to identify the dark material on both of these objects. Laboratory studies of the CO, CH<sub>4</sub>, and N<sub>2</sub> ices to develop better matches to the spectra should provide better insight into surface conditions.

REFERENCES AND NOTES

1. The data are from W. K. Hartman, D. Tholen, K. Meech, and D. P. Cruikshank [*Icarus* 83, 1 (1990)] for 2060 Chiron; B. E. Mueller, D. J. Tholen, W. K. Hartmann, and D. P. Cruikshank [*ibid.* 97, 150 (1992)] for 5145 Pholus; and D. Jewitt and J. Luu [*Nature* 362, 730 (1993)] for 1992 QB1. These three objects have diameters on the order of 200 km. The great comet of 1729 achieved naked-eye visibility although it never came closer to the sun than 4.0 AU [R. A. Lytleton, *The Comets and Their Origin* (Cambridge Univ. Press, Cambridge, 1953), p. 52; B. G. Marsden, *Catalogue of Cometary Orbits* (Minor Planet Center, Smithsonian Astrophysics Observatory, Cambridge, MA, 1986), ed. 5, p. 10].
2. D. P. Cruikshank *et al.*, *Science* 261, 742 (1993).
3. W. B. Hubbard, D. M. Hunten, S. W. Dieter, K. M. Hill, R. D. Watson, *Nature* 336, 452 (1988); J. L. Elliot *et al.*, *Icarus* 77, 148 (1989).
4. M. W. Buie and D. J. Tholen, *Icarus* 79, 23 (1989).
5. S. A. Stern, *Annu. Rev. Astron. Astrophys.* 30, 185 (1992).

6. Observations were as follows: 27 May 1992 (UT), 5:56 to 7:34 and 8:07 to 9:31 (UT), Charon phase 0.096; 28 May 1992 (UT), 6:25 to 8:08 and 9:00 to 9:20 (UT), Charon phase 0.255, where Charon phase 0 is near northern elongation and Charon phase 0.25 is near eastern elongation. The observations on 27 May had better signal to noise and received greater weight in the analysis.
7. D. P. Cruikshank, C. B. Pilcher, D. Morrison, *Science* **194**, 835 (1976).
8. W. J. Altenhoff *et al.*, *Astron. Astrophys.* **190**, 15 (1988); H. H. Aumann and R. G. Walker, *Astron. J.* **94**, 1088 (1987), M. V. Sykes, R. M. Cutri, L. A. Lebofsky, R. P. Binzel, *Science* **237**, 1336 (1987); E. F. Tedesco *et al.*, *Nature* **327**, 127 (1987).
9. K. A. Tryka, R. H. Brown, V. Anicich, D. P. Cruikshank, T. C. Owen, *Science* **261**, 751 (1993); W. Grundy, B. Schmitt, E. Quirico, *Icarus*, in press.
10. R. L. Marcialis, G. H. Rieke, L. A. Lebofsky, *Science* **237**, 1349 (1987).
11. M. W. Buie *et al.*, *Nature* **329**, 522 (1987).
12. D. J. Tholen and M. W. Buie, *Astron. J.* **96**, 1977 (1988).
13. Our models were calculated with the use of scattering theory developed by B. Hapke [*J. Geophys. Res.* **86**, 3039 (1981); *Icarus* **59**, 41 (1984); *ibid.* **67**, 264 (1986)]. In all of our calculations we derive the radiance factor at a phase angle of  $0^\circ$  ( $i = e = 0^\circ$ ). We assume isotropic surface scattering, a lunar-like regolith parameter for Hapke's  $h$  value, and make no corrections for macroscopic surface roughness. The continuum is defined as a series of straight line segments connecting local maxima such that data between maxima are not cut by the continuum. This definition eliminates absolute albedo information. However, preliminary calculations of geometric albedos for these mixtures are entirely consistent with the values derived from the telescopic data. We shifted the wavelengths of the optical constants to agree with the wavelength values for our observed Pluto spectrum before calculation of the spectra.
14. B. Schmitt, E. Quirico, E. Lellouch, *Proceedings of the Symposium on Titan*, Toulouse, France, 15 to 18 September 1991, publ. no. SP-338 (European Space Agency, Paris, 1992), p. 383; J. R. Green, R. H. Brown, D. P. Cruikshank, *Bull. Am. Astron. Soc.* **23**, 1208 (1991); G. B. Hansen, *Appl. Opt.* **25**, 2650 (1986); S. G. Warren, *ibid.* **23**, 1206 (1984); *Bull. Am. Astron. Soc.* **24**, 978 (1992).
15. The noisiness of the data in the short-wavelength wing of the 2.3- $\mu\text{m}$   $\text{CH}_4$  bands (Fig. 2) exemplifies the inadequacy of the available optical constants. This effect does not appear in our model for the Triton spectrum (2) because there is less  $\text{CH}_4$  in Triton's surface ices than in those of Pluto.
16. The shifting of the bands of  $\text{CH}_4$  diluted in  $\text{N}_2$  is related not only to the concentration. In particular, the band at 2.34  $\mu\text{m}$  shifts slightly and then splits as the  $\text{CH}_4$  concentration is reduced. Eventually the component of the band produced by pure methane diminishes in intensity as the 2.311- $\mu\text{m}$  component resulting from solution in  $\text{N}_2$  dominates the spectrum.
17. L. Trafton, *Astrophys. J.* **359**, 512 (1990). Eventually it should be possible to use the equation for nonideal solid solutions of  $\text{N}_2$  and  $\text{CH}_4$ , which have the form  $P_i = K \cdot X_i \cdot V_i$ , where  $K$  is a constant  $\geq 1$ ; no value for  $K$  is now available.
18. G. N. Brown, Jr., and W. T. Ziegler, *Adv. Cryog. Eng.* **25**, 662 (1980).
19. J. L. Elliot and L. A. Young, *Astron. J.* **103**, 991 (1992).
20. R. V. Yelle and J. I. Lunine, *Nature* **339**, 228 (1989).
21. Pluto's pressure scale height is  $55.7 \pm 4.5$  km (19).
22. R. V. Yelle, J. I. Lunine, D. M. Hunten, *Icarus* **89**, 347 (1991).
23. J. L. Elliot *et al.*, in preparation.
24. W. M. Irvine and R. F. Knacke, in *Origin and Evolution of Planetary and Satellite Atmospheres*, S. K. Atreya, J. B. Pollack, M. S. Matthews, Eds. (Univ. of Arizona Press, Tucson, 1989), pp. 3-34.
25. J. Geiss, *Astron. Astrophys.* **187**, 189 (1987).
- Rev. Mod. Astron.* **1**, 1 (1988).
26. T. Owen, *Astrophys. Space Sci.*, in press.
27. A. Bar-Nun and S. Chang, *J. Geophys. Res.* **88**, 6662 (1983).
28. E. Anders and N. Grevesse, *Geochim. Cosmochim. Acta.* **33**, 197 (1989).
29. A. L. Broadfoot *et al.*, *Science* **246**, 1459 (1989); G. L. Tyler *et al.*, *ibid.*, p. 1466.
30. The partial pressure of any additional species such as neon would have contributed to the

occultation determination of the refractivity scale height (19). This additional pressure would have forced us to lower our estimate of the surface temperature below that permitted by observations in order to reduce the pressure of  $\text{N}_2$  to accommodate the new species.

31. D. Lauffer, E. Kochavi, A. Bar-Nun, *Phys. Rev. B* **36**, 9219 (1987).

8 March 1993; accepted 2 June 1993

## The Phase Composition of Triton's Polar Caps

N. S. Duxbury and R. H. Brown

Triton's polar caps are modeled as permanent nitrogen deposits hundreds of meters thick. Complex temperature variations on Triton's surface induce reversible transitions between the cubic and hexagonal phases of solid nitrogen, often with two coexisting propagating transition fronts. Subsurface temperature distributions are calculated using a two-dimensional thermal model with phase changes. The phase changes fracture the upper nitrogen layer, increasing its reflectivity and thus offering an explanation for the surprisingly high southern polar cap albedo (approximately 0.8) seen during the Voyager 2 flyby. The model has other implications for the phase transition phenomena on Triton, such as a plausible mechanism for the origin of geyser-like plume vent areas and a mechanism of energy transport toward them.

Since the discovery of  $\text{N}_2$  on Triton (1), Neptune's largest moon, and especially since the Voyager flyby (2), there have been several attempts to model the transport of volatiles on Triton in response to its complex seasonal cycle (3). It has usually been assumed that the albedo distribution on Triton is the result of the seasonal  $\text{N}_2$  transport (4-8), but so far no models have successfully reproduced the observed albedo pattern.

An understanding of the mechanisms driving the albedo distribution is somewhat incidental to the question of the vertical phase composition of  $\text{N}_2$  ice deposits on Triton. Ground-based spectral measurements show that Triton's illuminated surface is mostly covered with frozen  $\text{N}_2$  at least many centimeters deep (1). The mean insolation on Triton is greatest at the equator and smallest at the poles (4, 5, 9). As a result, any  $\text{N}_2$  in excess of that which can be sublimated and recondensed during one of Triton's extreme seasons (3) is transported to permanent polar caps, which may be several hundred meters thick and extend as far toward the equator as  $\pm 45^\circ$  of latitude, depending on Triton's total inventory of surface  $\text{N}_2$  (8). The seasonal redistribution of volatiles also causes global temperature variations on time scales of a few tens of years (4, 5, 10), which can be as much as 15 to 20 K or as little as 2 to 4 K, depending again upon the total surface inventory of  $\text{N}_2$ . Furthermore, the 38 K temperature of

Triton's lower atmosphere is thought to be representative of all the  $\text{N}_2$  ice on Triton's surface (4, 5) and is perilously close to the temperature (35.61 K) of the  $\alpha$ - $\beta$  (cubic-hexagonal) phase transition in solid  $\text{N}_2$ .

The subsurface ice layer on Triton is therefore likely to experience the passage of multiple phase transition fronts as the global temperature oscillates above and below 35.61 K. Besides the absorption and liberation of latent heat at the phase transition, there is also a large change in volume over a small range in temperature: Laboratory measurements indicate that the density of solid  $\text{N}_2$  changes by 1 to 2% in a range of about 1 K around 35.61 K (11). The induced stresses cause severe fracturing of the crystalline solid when the transition is from the  $\beta$  to the  $\alpha$  phase (11). (To our knowledge, experiments to determine whether  $\alpha$ - $\text{N}_2$  crystals shatter when the phase transition is approached from lower temperatures have not been done; experiments (11) have dealt only with powdered  $\alpha$ - $\text{N}_2$  because large crystals are difficult to obtain.)

We assume that Triton is completely differentiated (2, 8), with a silicate core of radius  $\sim 1000$  km overlain by a water-ice mantle about 350 km thick and a thin veneer of solid  $\text{N}_2$ , no more than 1 km thick. We include in our heat transfer model the effect of the reversible phase transition from the denser cubic  $\alpha$  phase to the hexagonal  $\beta$  phase that occurs when the temperature rises to 35.61 K (for the  $^{14}\text{N}_2$  isotope at equilibrium vapor pressure), at which latent heat of 55.62 cal/mol for the  $^{14}\text{N}_2$  isotope (11) is absorbed. The

M.S. 183-501, Jet Propulsion Laboratory, California Institute of Technology, 4800 Oak Grove Drive, Pasadena, CA 91109.